Supporting Information

Coordinated regulation of heterochromatin inheritance by Dpb3-Dpb4 complex

Haijin He, Yang Li, Qianhua Dong, An-Yun Chang, Feng Gao, Zongxuan Chi, Min Su, Faben Zhang, Hyoju Ban, Rob Martienssen, Yu-hang Chen, & Fei Li

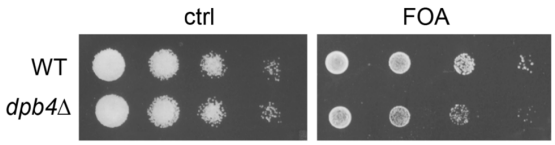

Fig. S1. Dpb4 is required for heterochromatin silencing. Serial dilutions of indicated cells harboring *ura4*$^{+}$ at the *otr* region were plated in medium containing 0.1% FOA. WT, wild type.

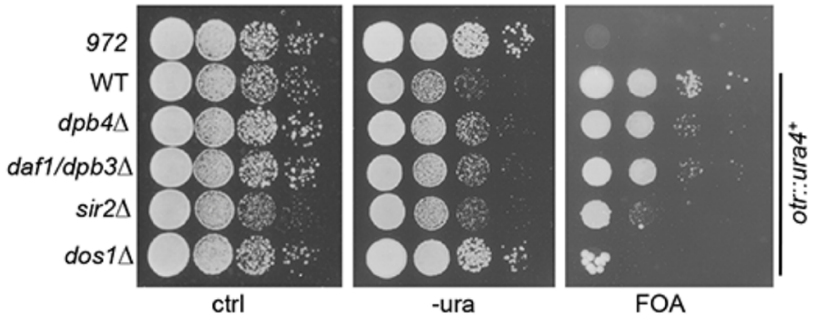

Fig. S2. Serial dilutions of indicated cells harboring *ura4*$^{+}$ at the *otr* region were plated in minimal medium without uracil (-ura) or medium containing FOA. WT, wild type. Strain 972, wild type strain harboring *ura4*$^{+}$ at the endogenous locus.

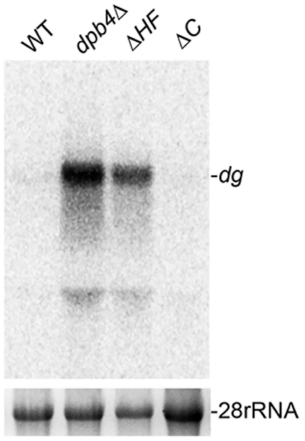

Fig. S3. Northern blotting analysis of transcript levels from the pericentromeric *dg* repeats in *dpb4-ΔHF* and *dpb4-ΔC* mutants. 28S rRNA was used as a loading control.

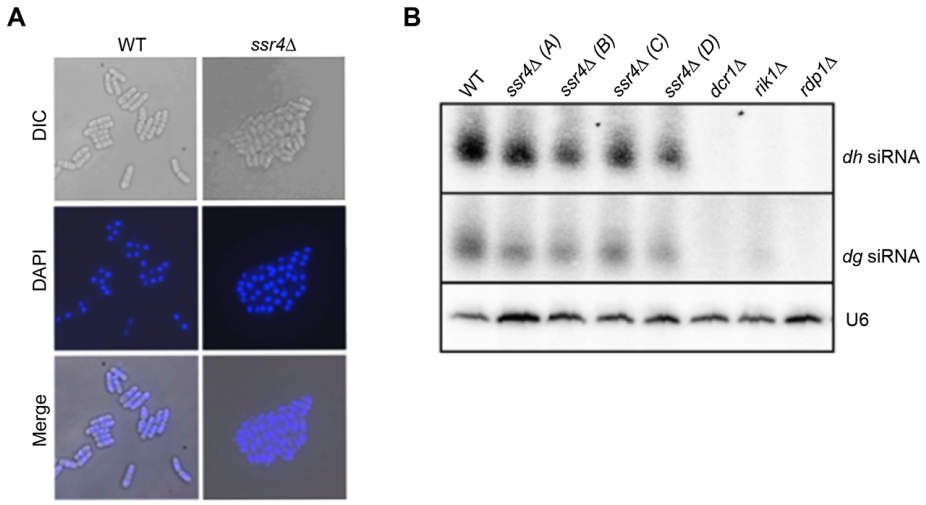

Fig. S4. Role of the SWI/SNF complex in heterochromatin silencing. (*A*) *ssr4Δ* mutant cells displays little growth defects. (*B*) Small RNAs from the pericentromeric regions are mildly reduced in *ssr4Δ* mutant. Total small RNAs were extracted from strains indicated. The blots were reprobed for U6 snRNA as a loading control.

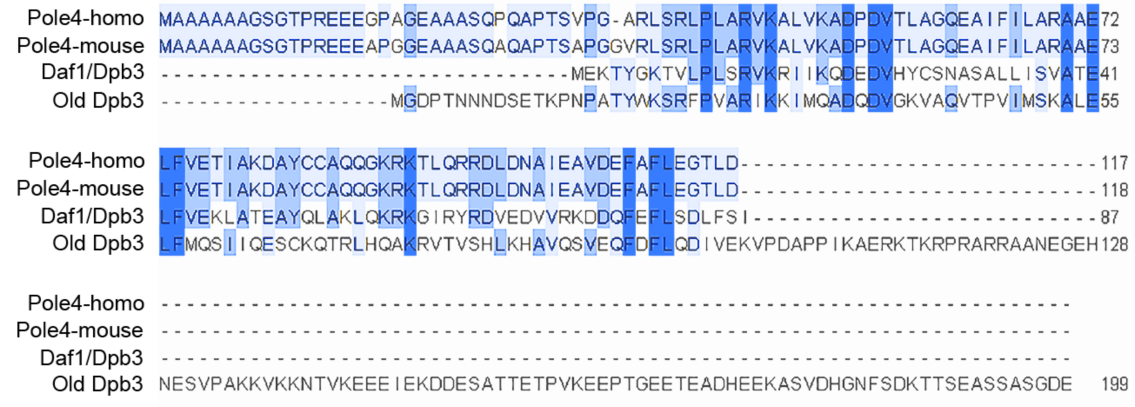

Fig. S5. Sequence analysis of the Daf1. Structure-based sequences alignment of Daf1 with human Pole4/Dpb3, mouse Pole4/Dpb3, and previously identified (old) Dpb3 (SPAC17G8.03c) in fission yeast.

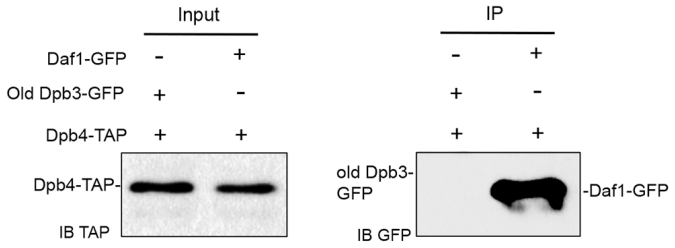

Fig. S6. Dpb4 is unable to interact with previously identified Dpb3. Cell lysates from cells expressing previously identified (old) Dpb3-GFP and Dpb4-TAP and from cells expressing Daf1-GFP and Dpb4-TAP were subjected to immunoprecipitation with an antibody specific for TAP. Precipitated proteins were analyzed by immunoblotting (IB) using a GFP antibody. Left: western blot analysis of input with an antibody for TAP.

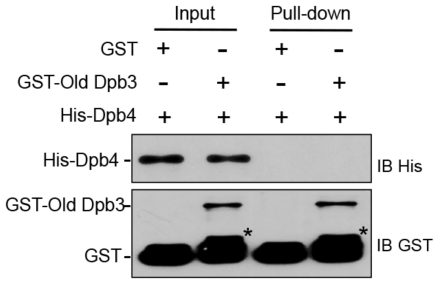

Fig. S7. GST pull-down assays revealed that the previously identified (old) Dpb3 was unable to interact with Dpb4. Both input and pull-down samples were subjected to immunoblotting with anti-His and anti-GST antibodies. *Degraded GST-Old Dpb3.

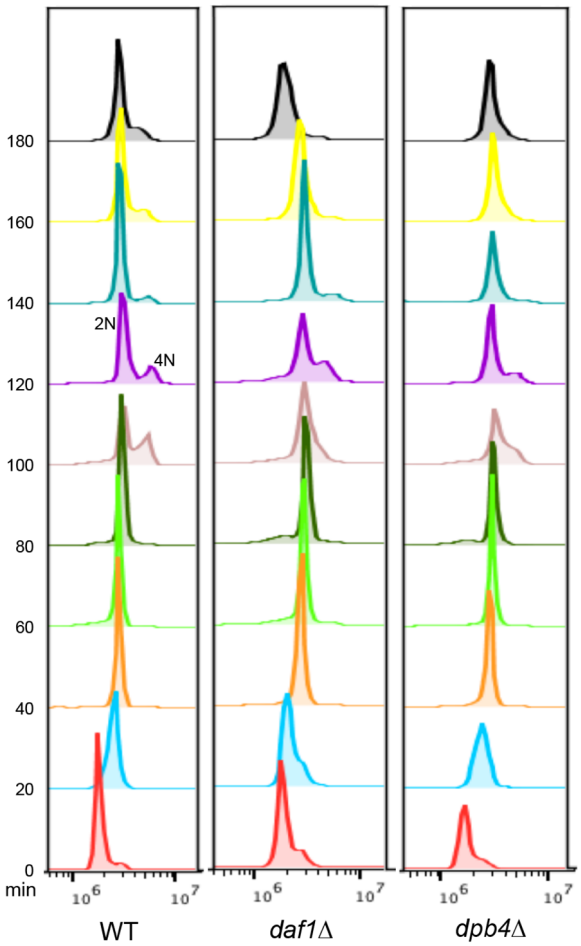

Fig. S8. *daf1*Δ and *dpb4*Δ mutants showed minor defects in S-phase progression. Cells were harvested every 20 minutes after release from hydroxyurea treatment, and processed for FACS analysis. In *S. pombe*, most S-phase cells are binucleate because cytokinesis does not take place until S phase is almost complete, resulting in 4N DNA content.

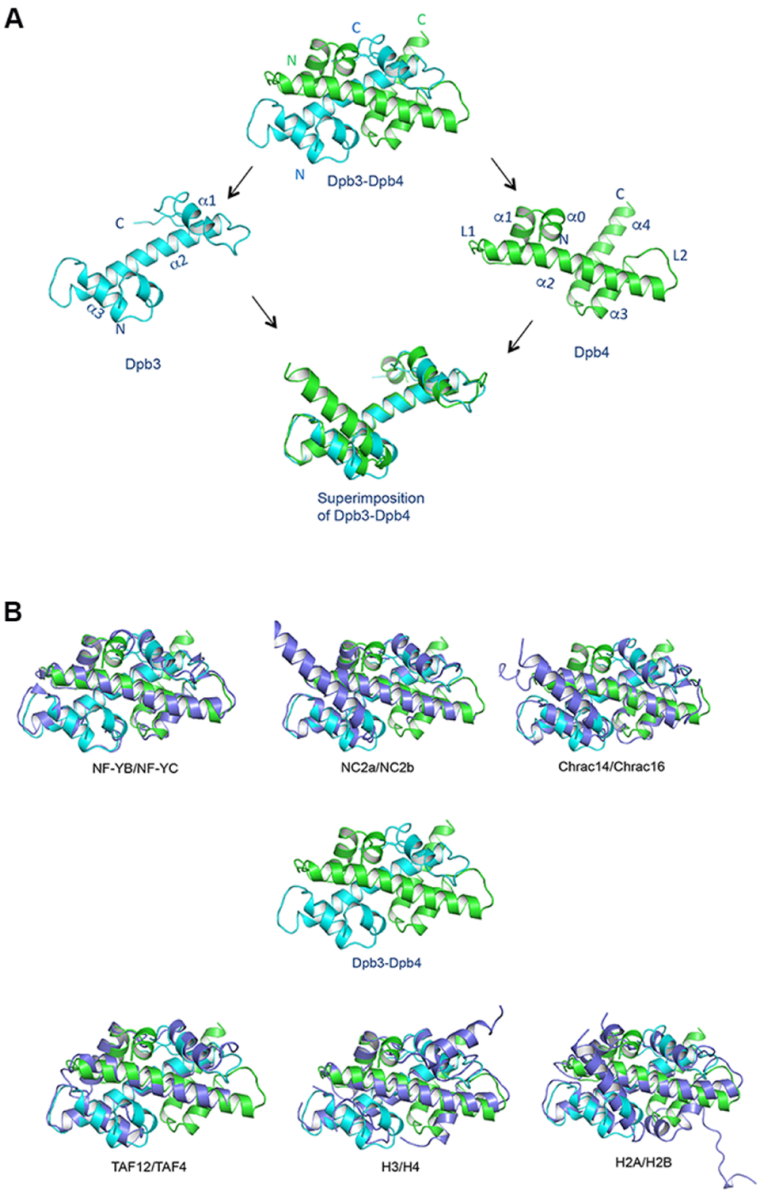

Fig. S9. Structure analysis of the Dpb3-Dpb4 complex. (*A*) Structural comparison of Dpb3 and Dpb4. Dpb3 is colored in cyan, and Dpb4 is colored in green. (*B*) Superimposition of the Dpb3-Dpb4 complex with other known histone fold pairs. Dpb3 is colored in cyan, and Dpb4 is colored in green. The other histone fold pairs are shown in slate.

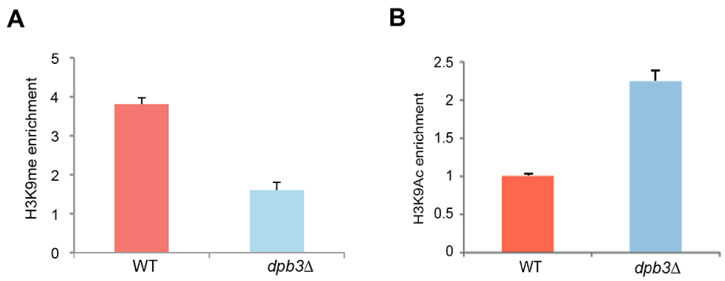

Fig. S10. Dpb3-Dpb4 is required for histone hypoacetylation and H3K9 methylation in heterochromatin. ChIP assays were performed using an antibody against H3K9 methylation (*A*) or H3K9 acetylation (*B*). Strains indicated carry *ura4*$^{+}$ at pericentromeric *otr* region. Immunoprecipitated products were amplified by primers specific for *ura4*$^{+}$. *act1*$^{+}$ was used as a control. Three independent experiments were performed. Error bars indicate SD.

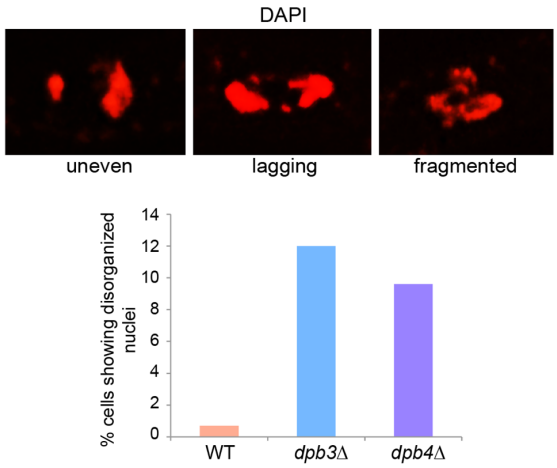

Fig. S11. Chromosome segregation defects in *dpb3Δ* cells, as shown by DAPI staining. Bottom: percentage of cells displaying disorganized nuclei in *dpb3*Δ and *dpb4*Δ.

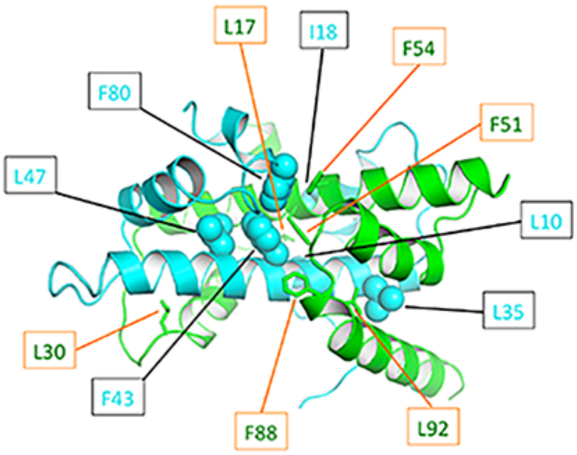

Fig. S12. Residues selected from the Dpb3-Dpb4 interface were mutagenized to alanine to disrupt the dimer interaction. Six residues in Dpb3 (L10/I18/L35/F43/L47A/F80) were shown as stick and colored in cyan; six residues in Dpb4 (L17/L30/F51/F54/F88/L92) were shown as sphere and colored in green.

Supporting Materials and Methods

Strains, Media and Genetic analysis

Fission yeast strains used in this study are listed in Table S2. Standard media and genetic analysis for fission yeast were used (1).

Mass spectrometry analysis

TAP-tag purification was performed as described (2). Briefly, cell lysates in 1× lysis buffer (50 mM bis-Tris propane, pH 7.0, 0.1 M KCl, 5 mM EDTA, 5 mM EGTA and 10% glycerol) were cleared by ultra-centrifugation. After the salt concentration was adjusted to 0.4 M KCl, the extract was incubated with IgG sepharose (Amersham Pharmacia Biotech) for 2 h. Immediately following washing, protein was eluted from the beads and incubated overnight with TEV protease (Invitrogen). S protein agarose beads (Novagen) was then added and incubated for 3 hr. The eluted fractions from S protein agarose were subjected to mass spectrometry analysis at Cold Spring Harbor Laboratory (New York, NY).

Co-immunoprecipitation

Immunoprecipitation was performed as described (3). Antibodies used include anti-GFP antibody (Roche, 11 814 460 001), an anti-myc antibody (Sigma, C3956), Peroxidase Anti-Peroxidase (P1291 SIGMA).

Protein Preparation

cDNAs encoding full-length Dpb3/Daf1 and Dpb4 were cloned into a modified plasmid pETDuet-1 and pET-24a (Novagen), respectively. Dpb3 was fused to a N-terminal 6X His-tag, and Dpb4 was followed by a C-terminal 10X His-tag with a TEV cleavage site. Large-scale protein production was performed using *E. coli* BL21 (DE3) cells grown in 2X YT medium containing Kanamycin (50 μg/ml) and Ampicillin (100 μg/ml). The target protein complex was purified to homogeneity by using a combination of Ni^{2+} affinity chromatography, His-tag removal by TEV, and Superdex 200 gel filtration chromatography.

Crystallization and Structure Determination

The purified Se-Met Dpb3-Dpb4 complex was concentrated to ~8 mg/ml and was crystallized using an under-oil method with a reservoir solution containing 10% (W/V) PEG3350，100mM CHES (pH 9.5). Micro-seeding was required for growth of crystals to suitable sizes for diffraction experiments. Cryo-protection was achieved by sequential addition of increments of mother liquor supplemented with 25% w/v glycerol, followed by flash freezing in liquid nitrogen.

Crystals of the Dpb3-Dpb4 complex grew in space group $P6_5$ with a=b=86.5Å, c=59.8Å and α=β=90º, γ=120º. The structure was determined by the single-wavelength anomalous diffraction (SAD) method with data collected at the wavelength of 0.97853 Å at the beam-line BL19U of the Shanghai Synchrotron Radiation Facility (SSRF). Assessment of data quality for phasing, location of heavy atom sites and phases were calculated using the SHELX programs. All the secondary structure elements were clearly visible in the experimental electron density map. The model was initially built with Autobuild in Phenix package, and further completed manually in Coot. The final model was refined to 1.9 Å with phenix.refine in the Phenix. Structure validation was performed with PROCHECK. Data collection and refinement statistics are summarized in Table S1. All structural figures were prepared in PyMOL (http://www.pymol.org). The atomic coordinates have been deposited in the Protein Data Bank (PDB; accession code: 5Y26 and 5Y27).

***in vitro* pull-down assays**

in vitro pull-down assays were performed as previously described (4). Briefly, purified bait protein was immobilized in 20 µl Glutathione Sepharose beads (GE), and incubated with purified prey protein for 2 h at 4°C. The beads were then washed three times with buffer containing 50 mM Tris pH 8.0, 100mM NaCl and 2% glycerol. The pull-down protein was subsequently analyzed by SDS-PAGE.

Mutational Studies on the Dimer Interface

The genes for the Dpb3-6A (L10A/I18A/L35A/F43A/L47A/F80A) and Dpb4-6A (L17A/L30A/F51A/F54A/F88A/L92A) mutants were synthesized, and confirmed by sequencing. Dpb3 and the Dpb3-6A mutant were cloned individually into a modified plasmid E2, which generates a His-SUMO fusion protein. Dpb4 and Dpb4-6A mutant were cloned into the pGEX-6P-1 vector and expressed as a GST fusion protein. The expression and purification for the proteins were conducted as previously described (4).

Fluorescence activated cell scan (FACS) analysis

S. pombe cells were synchronized in early S phase by treating exponentially growing cells with 15 mM hydroxyurea for 4 hours. After release to the rich YES media, samples were collected every 20 minutes up to 3 hours. DNA content of cells were stained with SYTOX Green (Molecular Probes, Eugene, OR) and analyzed using a Becton Dickinson FACSAria (Department of Biology, New York University).

ChIP

ChIP was performed by as described (3). The ChIP samples were analyzed using duplex PCR using primers listed in Table S3. Quantitations were performed using ImageJ 1.46r software. All experiments were independently repeated three times.

Northern Blot

Northern blot was performed according to the standard protocol. Briefly, RNA samples were purified using Trizol (Invitrogen). 5 µg total RNA from each sample were loaded to a formaldehyde gel, separated and transferred to an Amersham Hybond-N+ membrane in 2X SSC buffer. After UV cross-linking, the membranes were hybridized by ^{32}P-labeled probe recognizing pericentromeric heterochromatin or 28S rRNA as a control, and exposed to film for autoradiography.

RT-PCR

RT-PCR was performed as described previously (5). Briefly, total RNA was isolated from cells growing at log phase by RNeasy mini kit (Qiagen). After treated with DNAase I (Promega), 50 ng of purified RNA was analyzed by RT-PCR in a 25 µl reaction volume using a one-step RT-PCR kit (Qiagen). Equal loading of RNA samples were assessed by amplification of the control gene, *act1*$^{+}$. Primers used for RT-PCR are listed in Table S3.

Small RNA Northern Blot

Small RNA Northern Blot was performed as described (5). Briefly, siRNAs were extracted from exponentially growing cells in YES media using a mirVana miRNA isolation kit (Ambion). 25 µg of small total RNA was resolved by a 15% denaturing acrylamide gel, and blotted to a charged nylon membrane (Hybond-N+, Amersham). RNA blots were cross-linked and hybridized with DNA probes specific for centromere *otr* region or U6 snRNA as a loading control.

Table S1. Data collection and refinement statistics.

Parameter*	Se-Met	Native
Data collection statistics		
Wavelength (Å)	0.97915	0.97853
Resolution range (Å)	37.37-1.90 (1.97-1.90)	43.26 -2.00 (2.07-2.00)
Space group	P 65	P 65
Cell dimensions		
a,b,c (Å)	86.29 86.29 59.71	86.52 86.52 59.80
α, β, ɣ (°)	90, 90, 120	90, 90, 120
Unique reflections	20057 (2014)	16636 (1580)
Multiplicity	49.9 (50.0)	15.1 (13.7)
Completeness (%)	99.87 (98.92)	97.8 (99.5)
Mean I/sigma(I)	39.7 (6.7)	23.2 (3.4)
Wilson B-factor	17.0	24.9
R-merge (%) †	6.3 (71.3)	9.1(66.1)
Structure refinement		
Rwork/Rfree (%)	19.2/24.4	18.1/22.4
Number of non-hydrogen atoms	1749	1671
macromolecules	1523	1527
ligands	6	6
waters	220	138
Protein residues	190	189
RMSD		
Bond length (Å)	0.008	0.008
Bond angles (°)	1.02	0.99
Average B-factor	27.0	39.7
Ramachandran plot (%)		
favored region	99	98
Outliers region	0	0.53

*Values in parentheses are for highest-resolution shell.

† Rmerge= Σhkl |I-<I>|/ΣhklI where I is the intensity of unique relfection hkl and <I> is the average over symmetry-related observations of unique reflection hkl.

Table S2. Strains used in this study.

FL 24	*h^{+} otr1R(SphI)::ura4^{+} leu1-32 ade6-210 ura4-DS/E his1-10*
FL 78	*h^{90} otr1R(SphI)::ade6^{+} tel1L-his3^{+} tel2L-ura4^{+} leu1-32 ade6-210 his3-D1 ura4-DS/E*
FL 97	*h^{90} mat3M::ura4^{+} leu1-32 ade6-210 ura4-DS/E*
FL701	*h^{-} dpb4Δ::kan leu1-32 ade6-210 ura4-D18*
FL702	*h^{+} dpb4Δ::kan otr1R(SphI)::ura4^{+} leu1-32 ade6-210 ura4-(DS/E or D18?)*
FL703	*h$^{?}$ dpb4-ΔHF::kan otr1R(SphI)::ura4^{+} leu1-32 ade6-210 ura4-(DS/E or D18?)*
FL704	*h$^{?}$ dpb4-ΔC::kan otr1R(SphI)::ura4^{+} leu1-32 ade6-210 ura4-(DS/E or D18?)*
FL705	*h^{+} dpb4::dpb4-TAP-kan leu1-32 ade6-210 ura4-D18*
FL706	*h^{-} daf1::daf1-GFP-ura4^{+} leu1-32 ade6-210 ura4-D18*
FL707	*h^{+} daf1Δ::kan leu1-32 ade6-210 ura4-D18*
FL708	*h^{+} daf1Δ::kan otr1R(SphI)::ura4^{+} leu1-32 ade6-210 ura4-(DS/E or D18?)*
FL709	*h$^{?}$ daf1Δ::kan otr1R::ade6^{+} leu1-32 ade6-210*
FL710	*h$^{?}$ daf1Δ::kan mat3M::ura4^{+} leu1-32 ade6-210 ura4-(DS/E or D18?)*
FL711	*h$^{?}$ daf1Δ::kan tel2L::ura4^{+} leu1-32 ade6-210 ura4-(DS/E or D18?)*
FL715	*h$^{?}$ dpb4Δ::ura GFP-swi6::LEU2 leu1-32 ade6-210 ura4-D18*
FL716	*h$^{?}$ daf1Δ::kan GFP-swi6::LEU2 leu1-32 ade6-210 ura4-D18*
FL721	*h$^{?}$ ssr4Δ::kan leu1-32 ade6-210 ura4-D18*
FL722	*h$^{?}$ sir2::sir2-myc-kan dpb4::dpb4-TAP-kan*
FL723	*h$^{?}$ dpb4::dpb4-TAP-kan daf1::daf1-GFP-ura4^{+} leu1-32 ade6-210 ura4-D18*
FL724	*h^{-} sir2Δ::kan otr1R(SphI)::ura4^{+} ura4-(DS/E or D18?)*
FL725	*h$^{?}$ dos1Δ::kan otr1R(SphI)::ura4^{+} leu1-32 ade6-210 ura4-(DS/E or D18?)*
FL726	*h$^{?}$ dpb4Δ::kan sir2Δ::kan otr1R(SphI)::ura4^{+} ura4-(DS/E or D18?)*
FL727	*h$^{?}$ daf1Δ::kan sir2Δ::kan otr1R(SphI)::ura4^{+} ura4-(DS/E or D18?)*
FL737	*h^{90} dpb3::dpb3-GFP-HA-kan leu1-32 lys1-131 ade6-216 ura4-D18*
FL738	*h$^{?}$ dpb4::dpb4-TAP-kan dpb3::dpb3-GFP-HA-kan leu1-32 ura4-D18*
FL741	*h^{-} daf1::daf1-6A-GFP-LEU2 leu1-32 ade6-210 ura4-D18*
FL742	*h$^{?}$ daf1::daf1-6A-LEU2 otr1R(SphI)::ura4^{+} leu1-32 ade6-210 ura4-(DS/E or D18?)*
FL743	*h$^{?}$ cdc20::cdc20-2×FLAG-kan daf1::daf1-GFP-ura4^{+} leu1-32 ade6-210 ura4-D18*
FL744	*h^{-} cdc20::cdc20-2×FLAG-kan daf1::daf1-6A-GFP-LEU2 leu1-32 ade6-210 ura4-D18*
FL745	*h^{-} dpb4::dpb4-TAP-kan daf1::daf1-6A-GFP-LEU2 leu1-32 ade6-210 ura4-D18*

Table S3. Primers used in this study.

Primer name	Sequence
Act-1	ATGGAAGAAGAAATCGCAGCG
Act-2	ATGCCAAATCTTTTCCATATC
RT1	GAAAACACATCGTTGTCTTCAGAG
RT2	CGT CTT GTA GCT GCA TGT GAA

Supporting References

1. Moreno S, Klar A, & Nurse P (1991) Molecular genetic analysis of fission yeast Schizosaccharomyces pombe. *Methods Enzymol* 194:795-823.
2. Cheeseman IM*, et al.* (2001) Implication of a novel multiprotein Dam1p complex in outer kinetochore function. *J Cell Biol* 155(7):1137-1145.
3. Li F, Martienssen R, & Cande WZ (2011) Coordination of DNA replication and histone modification by the Rik1-Dos2 complex. *Nature* 475(7355):244-248.
4. Dong Q*, et al.* (2016) Ccp1 Homodimer Mediates Chromatin Integrity by Antagonizing CENP-A Loading. *Mol Cell* 64(1):79-91.
5. Li F*, et al.* (2005) Two novel proteins, Dos1 and Dos2, interact with Rik1 to regulate heterochromatic RNA interference and histone modification. *Current Biology* 15(16):1448-1457.